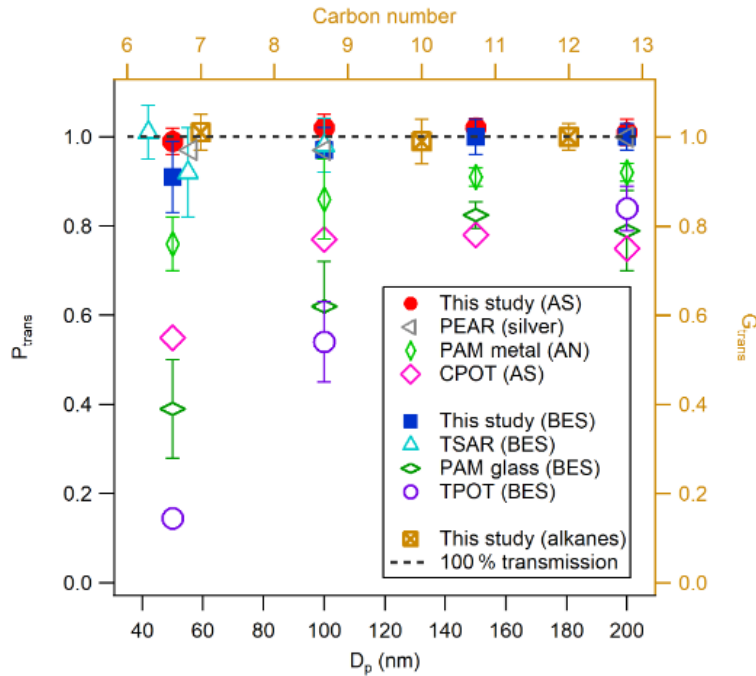


Xu and Collins present the evaluation of a custom PFA OFR design by performing characterization studies that included measurements of residence time distributions, gas and particle transmission efficiencies, yields of laboratory SOA generated from OH oxidation of  $\alpha$ -pinene and m-xylene, and ambient secondary aerosol (SA) formation following OH exposure in the PFA OFR. Given the emergence of OFRs as a technique to characterize SA formation, I might support eventual publication of this manuscript in AMT after my comments below are taken into consideration.

### **General Comments**

1. There is a growing body of literature suggesting that adding 185 nm irradiation in OFRs – along with 254 nm – is advantageous to use of only 254 nm radiation with externally added ozone, especially with respect to organic peroxy radical ( $\text{RO}_2$ ) chemistry, resilience to OH suppression and UV photolysis, and easier operation in the field (e.g. Peng et al., 2019; Peng and Jimenez, 2020; Rowe et al., 2020). It isn't clear to me from the text (L137-L141, L151-L155) if the PFA OFR can implement the OFR185 mode or not. If OFR185 operation is possible, it's worth clarifying that, and explaining why it wasn't evaluated here. If it is not possible, please clarify, and discuss the associated tradeoffs.
2. Overall, the most novel aspect of the PFA OFR design appears to be the higher reflectivity achieved with the ePTFE gasket combined with the lower lamp power. This design modification enables the PFA OFR to achieve a higher OH exposure at a specific lamp power relative to other designs, as noted in L128-L130, which is noteworthy. The potential implications that are identified from the results seem to be better residence time distributions because of less recirculation and reduced temperature gradients. Aside from that, the implication on measurements of interest was less clear. The gas and penetration efficiencies are comparable to previous OFR designs with broader RTDs and less internal reflectivity, as are the  $\alpha$ -pinene and m-xylene SOA yields. To me, this suggests that results of the sort described here are not sensitive to this design component, or that OFR applications that might be affected by higher internal reflectivity are not adequately discussed. I would strongly encourage adding a section that illustrates applications where this higher reflectivity demonstrably improve performance using metrics other than the OH exposure.
3. The comparison of particle penetration efficiencies is incomplete, and in some places is misleading. Figure 7 shows that the size-dependent particle penetration efficiencies of PFA, PAM and TPOT OFRs, and as presented, suggests that the PFA performance is the best of the three. However, as noted in L215-L220, the PFA was conditioned for 12 hours prior to testing to suppress static discharge, whereas the other OFRs were not. Thus, results are a combination of OFR design and testing procedure, and how to isolate the relative importance of each factor is not clear. Either results for the PFA prior to conditioning also need to be shown for a direct comparison, or this difference needs to be more clearly identified in the figure/caption. Figure 7 also does not show published particle transmission efficiency data for several other OFR designs that were already referenced in this paper. Please see Figure 2 from Li et al., 2019, reproduced below for reference; to my knowledge, this is the most comprehensive comparison to date:



**Figure 2.** Particle (left and bottom axis) and gas (right and top axis) transmission efficiencies ( $P_{\text{trans}}$  and  $G_{\text{trans}}$ ) for the ECCC-OFR. Particle transmission efficiencies of other OFRs are shown for comparison: PAM glass and TPOT (Lambe et al., 2011), PAM metal (Karjalainen et al., 2016), TSAR (Simonen et al., 2017), CPOT (Huang et al., 2017), and PEAR (Ihalainen et al., 2019).

4. Similarly, the gas penetration efficiency may have been measured in different ways. For example, in measurements by Lambe et al. (2011) and Li et al. (2019), the OFR walls were first passivated by flowing the relevant gas(es) through the OFR. Based on the text (L199-L200), it doesn't appear that that was done here, in which case this may be a plausible explanation for the lower  $\text{SO}_2$  penetration efficiency in the PFA OFR.
5. Occasionally the reactor is referred to as "PFA". It might be less ambiguous to refer to it as the "PFA OFR" to distinguish it from perfluoroalkoxy alkanes.

#### Technical Comments

6. L148-L150: The authors state that "Continuous operation for 6 hours resulted in a temperature rise of less than 2°C" What is the temperature rise over 24 hours or longer, i.e. periods that would be relevant for continuous ambient OFR measurements?.
7. L168: Please mention the OD of the copper bypass line, clarify the reason for using a 150 cm length of bypass inlet versus 200 ccm length of OFR inlet, and calculate the residence time in the bypass and OFR inlet lines to place in context of the OFR residence time.

8. L313: Were different side flow:center flow ratios studied to evaluate the influence of this flow ratio on the residence time distribution? Is a side:center flow ratio of 1:1 optimal, or could the RTD be further improved at a different value?
9. L356: This statement is not correct – the TPOT and PAM OFRs were also operated in OFR254 mode in the study described here.
10. L412-L414, L423-425: Please apply the OFR254 OH exposure estimation equation developed in Section 3.7 of Peng et al. (2015) to calculate the OH exposure during these SOA yield measurements. As far as I can tell, the required inputs to this equation are available from the measurements that were described here.
11. Figure 1 and Section 2.1: Please explain/justify the use of 35° and 24° inlet and outlet cone angles.
12. Figure 3 should either be moved to Supplement or deleted and described briefly in words.
13. Figure 4 could be moved to Supplement.
14. Figure 6a: it would be better to present results in terms of the photon flux, which is an intrinsic property of the OFR that could be more easily compared with other OFR designs, rather than the fractional lamp power, which is only applicable to the specific lamp type used here. The photon flux could be estimated from the maximum lamp output normalized by the internal surface area of the OFR, or, preferably, constrained using ozone measurements measured at the exit of the OFR (as a function of humidity and lamp power) using a photochemical model such as the OFR-KinSim mechanism (Peng and Jinenez, 2019, 2020). Also, please change the y-axis to a logarithmic scale, or make the y-axis scale go to zero.
15. Figure 6b: I don't understand the utility of showing the single point obtained without ePTFE at 50% lamp power. With only 2-3 data points shown here, it might just be easier to integrate this data into Figure 6a.
16. Figure 7 is incomplete (see comment #3).
17. Figure 8: Please clarify whether the literature data shown here were obtained with UV lamps on or off.
18. Figure 9 could be moved to Supplement.
19. Figure 10 could be moved to Supplement.
20. In my opinion, Figure 11 should plot the SOA yield as a function of OH exposure rather than  $C_{OA}$ . The precursor concentration was not systematically varied, and  $C_{OA}$  is not really the independent variable here. The OH exposure can be estimated using the OFR254 estimation equation provided by Peng et al. (2015).

21. Figure 13 could be moved to Supplement.

## **References**

Li, K., Liggio, J., Lee, P., Han, C., Liu, Q., and Li, S.-M.: Secondary organic aerosol formation from  $\alpha$ -pinene, alkanes, and oil-sands-related precursors in a new oxidation flow reactor, *Atmos. Chem. Phys.*, 19, 9715–9731, <https://doi.org/10.5194/acp-19-9715-2019>, 2019.

Z. Peng, D.A. Day, H. Stark, R. Li, B.B. Palm, W.H. Brune, and J.L. Jimenez. HO<sub>x</sub> radical chemistry in oxidation flow reactors with low-pressure mercury lamps systematically examined by modeling. *Atmos. Meas. Tech.*, 8, 4863-4890, doi:10.5194/amt-8-4863-2015, 2015.

Z. Peng and J. L. Jimenez. KinSim: A Research-Grade, User-Friendly, Visual Kinetics Simulator for Chemical-Kinetics and Environmental-Chemistry Teaching, *J. Chem. Educ.* 2019, 96, 4, 806–811. <https://pubs.acs.org/doi/10.1021/acs.jchemed.9b00033>.

Z. Peng, J. Lee-Taylor, J.J. Orlando, G.S. Tyndall, J.L. Jimenez. Organic peroxy radical chemistry in oxidation flow reactors and environmental chambers and their atmospheric relevance. *Atmos. Chem. Phys.*, 19, 813-834, 2019, <https://doi.org/10.5194/acp-19-813-2019>.

Z. Peng, J.L. Jimenez. Radical chemistry in oxidation flow reactors for atmospheric chemistry research. *Chem. Soc. Rev.*, 49, 2570-2616, doi: 10.1039/C9CS00766K, 2020.

Rowe, J. P., Lambe, A. T., and Brune, W. H.: Technical Note: Effect of varying the  $\lambda = 185$  and 254 nm photon flux ratio on radical generation in oxidation flow reactors, *Atmos. Chem. Phys.*, 20, 13417–13424, <https://doi.org/10.5194/acp-20-13417-2020>, 2020.